(Tokyo) 79, 1007–1012.
Ohnishi, M., Yamashita, T., & Hiromi, K. (1977) J. Biochem. (Tokyo) 81, 99–105.
Phillips, D. C. (1966) Sci. Am. 215 (Nov), 78.
Sakoda, M., & Hiromi, K. (1976) J. Biochem. (Tokyo) 80, 547–555.
Shimahara, K., & Takahashi, T. (1970) Biochim. Biophys. Acta 201, 410–415.
Tanaka, A., Ohnishi, M., & Hiromi, K. (1981) Biochemistry (following paper in this issue).

Stopped-Flow Kinetic Studies on the Binding of Gluconolactone and Maltose to Glucoamylase†

Akiyoshi Tanaka, Masatake Ohnishi, and Keitaro Hiromi*

ABSTRACT: The binding of the transition-state analogue gluconolactone and a substrate maltose to *Rhizopus niveus* glucoamylase was studied kinetically by using the stopped-flow method by monitoring the decrease in the enzyme fluorescence, in relation to the subsite structure of the enzyme [Hiromi, K. (1970) *Biochem. Biophys. Res. Commun. 40*, 1–6]. The binding kinetics of both ligands (represented by L) agreed well with a two-step mechanism which consists of a fast bimolecular process followed by a slow unimolecular process:

$$E + L \underset{k_{-1}}{\overset{k_{+1}}{\rightleftharpoons}} EL \underset{k_{-2}}{\overset{k_{+2}}{\rightleftharpoons}} EL^*$$

where EL and EL* are the enzyme–ligand complexes loosely bound and tightly bound, respectively. In each case, the observed fluorescence intensity decrease of the enzyme protein was confirmed to be accompanied solely with the slow unimolecular process. A competitive inhibitor glucose, which is considered to bind predominantly to subsite 2 (the second subsite counted from the terminal subsite to which the nonreducing-end glucose residue of substrate is bound in a productive mode), inhibits only the fast bimolecular process for the maltose binding. On the other hand, for the gluconolactone binding, glucose inhibits the fast bimolecular process and the k_{-2} step, but not the k_{+2} step, in the unimolecular process. These results are most reasonably accounted for by the following mechanism: In the fast bimolecular process of the binding, gluconolactone transiently binds to subsite 2 and maltose to subsites 2 and 3, and in the unimolecular process, they relocate to subsite 1 and subsites 1 and 2, respectively, accompanied by the decrease in fluorescence intensity. The fluorescence change may be caused by the microenvironmental change of a tryptophan residue located at subsite 1.

Glucoamylase[1] hydrolyzes the nonreducing-end glucosidic bond of starch. To this enzyme the subsite theory was successfully applied quantitatively (Hiromi, 1970; Hiromi et al., 1973).

The fluorescence intensity of the enzyme protein is decreased by the binding of substrates or analogues, and the binding of ligands with the enzyme was investigated by the static and the kinetic method with the decrease in the enzyme fluorescence as a probe (Hiromi et al., 1974; Ohnishi et al., 1977).

In the preceding paper (Hiromi et al., 1981), we investigated the binding states of gluconic acid 1,5-lactone (gluconolactone) and glucose by the fluorometric titration at equilibrium. It would be reasonably concluded that gluconolactone binds to subsite 1 of the enzyme (the terminal subsite at which the nonreducing-end glucose residue of substrate is situated in the productive binding mode) and that glucose predominantly binds to subsite 2.

The static method, however, cannot provide any information about elementary processes of the ligand binding. To obtain such mechanistic information, it is necessary to use the transient kinetics with fast reaction techniques. In this paper, we aimed to elucidate kinetically the elementary processes in the binding of two ligands, a transition state analogue gluconolactone and a substrate maltose, to the enzyme by using the fluorescence stopped-flow method.

Experimental Procedures

Materials. Glucoamylase, gluconic acid 1,5-lactone (simply referred to as gluconolactone), and glucose were the same as those described in the preceding paper (Hiromi et al., 1981). Maltose was purchased from Nakarai Chemicals Co., Ltd., and was confirmed to be pure by the paper chromatographic method (Robyt & French, 1963). Gluconolactone was used within 5 min after its dissolution to minimize its hydrolysis into gluconic acid and conversion into gluconic acid 1,4-lactone (Shimahara & Takahashi, 1970). Maltose and glucose solutions were kept at the experimental temperature for 5 h or more before use to complete anomeric equilibration.

Methods. Binding kinetics of ligands to the enzyme was studied by monitoring the fluorescence intensity decrease of the enzyme protein by the stopped-flow method. The time course of the binding reactions was observed with a gas pressure driven type stopped-flow apparatus (Union Giken RA-401) (Hiromi, 1979) with a 200-W D_2 lamp as the light source. The change in the fluorescence intensity (excited at 280 nm throughout the experiment) was observed through a cutoff filter (Toshiba Kasei Kogyo, UV-31; 50% transmittance at 310 nm) from the right angle to the incident beam. With the quartz cell used (2-mm-inner diameter), the dead time of the apparatus was determined to be 0.9 ms under the operating condition (6 kg/cm^2 nitrogen gas pressure for driving) according to the method with ascorbic acid and 2,6-dichloro-

† From the Department of Food Science and Technology, Faculty of Agriculture, Kyoto University, Kyoto 606, Japan. *Received April 28, 1981.* This work was supported in part by a grant-in-aid for Scientific Research from the Ministry of Education, Science and Culture of Japan (No. 447094).

[1] Abbreviations used: E or glucoamylase, 1,4-α-D-glucan glucohydrolase from *Rhizopus niveus* (EC 3.2.1.3); L or gluconolactone, gluconic acid 1,5-lactone; G, glucose; M, maltose.

0006-2960/82/0421-0107$01.25/0

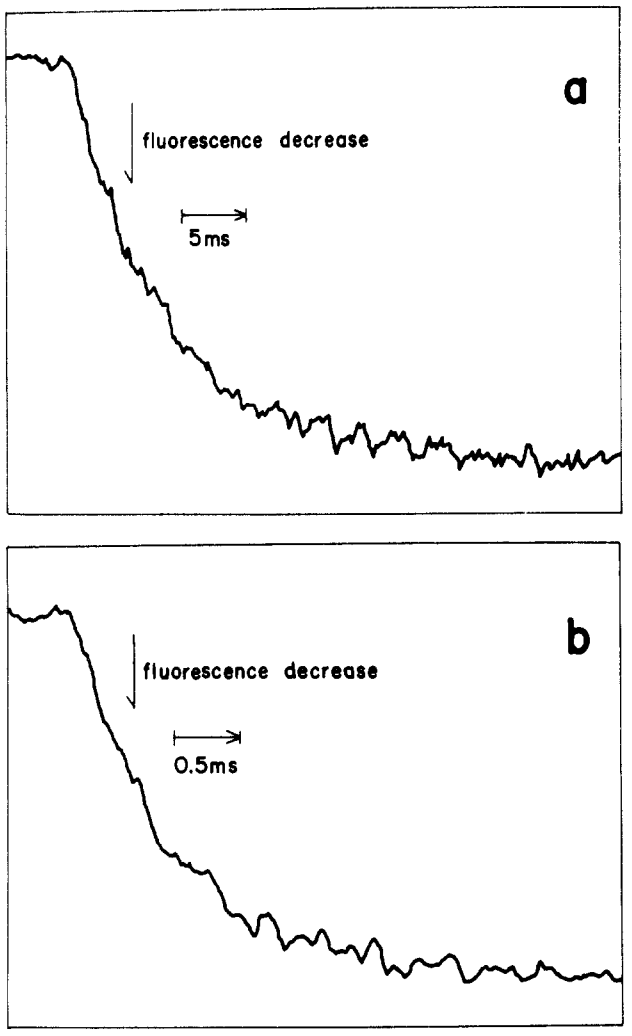

FIGURE 1: Typical time course of the fluorescence intensity decrease caused by the binding of gluconolactone (a) and maltose (b) to the enzyme. Excitation wavelength λ_{ex} = 280 nm; 9 times accumulation. (a) $[Glucoamylase]_0$ = 6.1 μM and $[gluconolactone]_0$ = 7.5 mM, pH 4.5, 10 °C; (b) $[glucoamylase]_0$ = 13.1 μM and $[maltose]_0$ = 15 mM, pH 4.5, 5 °C. (Concentrations refer to those in the reaction mixture throughout.)

phenolindophenol (Tonomura et al., 1978; Nakatani & Hiromi, 1980). Reaction curves were accumulated usually 9 times by using a data-averaging processor (Union Giken RA-450) to improve the signal to noise ratio. The enzyme concentration in the reaction mixture was fixed at 6.1 μM for the enzyme–gluconolactone system and at 13.1 μM for the enzyme–maltose system. The concentration ranges of the ligands were 0.02–60 mM for gluconolactone and 0.05–30 mM for maltose. All the experiments were carried out in 0.02 M acetate buffer, pH 4.5, and at 10 (for gluconolactone) or 5 °C (for maltose) unless otherwise specified.

Results

Binding of Gluconolactone to Glucoamylase. Figure 1a shows a typical example of the reaction curves for the binding of the enzyme with gluconolactone at 10 °C. Over the concentration range of gluconolactone used, only one relaxation was obeyed, and this showed apparent first-order kinetics. The apparent first-order rate constant k_{app} (or reciprocal of the relaxation observed, $1/\tau$) was evaluated from the Guggenheim plot (Guggenheim, 1926).

Figure 2a shows the dependence of k_{app} on the initial concentration of gluconolactone $[L]_0$. This hyperbolic dependence of k_{app} on $[L]_0$ cannot be explained by a simple one-step

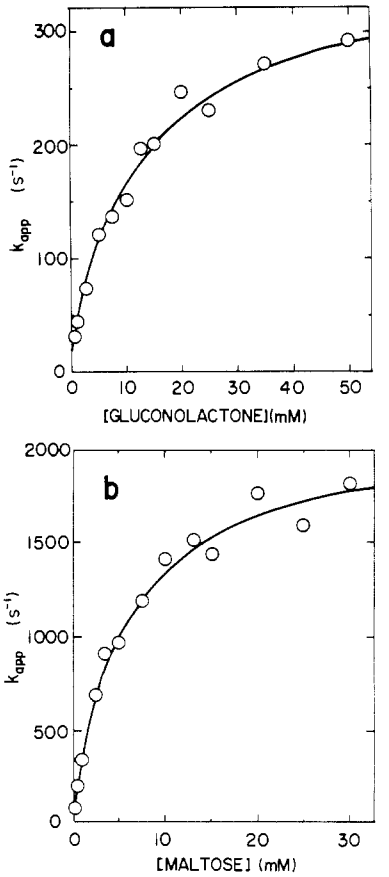

FIGURE 2: Dependence of the apparent first-order rate constant k_{app} on the initial concentrations of gluconolactone (a) and maltose (b). (a) The solid line is the theoretical curve obtained according to eq 3 with K_{-1} = 14 mM, k_{+2} = 350 s^{-1}, and k_{-2} = 22 s^{-1}. (b) The solid line is the theoretical curve obtained according to eq 8 with K_{-1} = 5.6 mM, k_{+2} = 2030 s^{-1}, and k_{-2} = 45 s^{-1}.

mechanism; E + L $\rightleftarrows$ EL, where E, L, and EL represent the enzyme, gluconolactone, and the enzyme–gluconolactone complex, respectively. The experimental results are consistent with those expected from a two-step mechanism, which involves a fast bimolecular binding process followed by a slow unimolecular isomerization process (Eigen & DeMayer, 1963; Bernasconi, 1976):

$$E + L \underset{k_{-1}}{\overset{k_{+1}}{\rightleftarrows}} EL \underset{k_{-2}}{\overset{k_{+2}}{\rightleftarrows}} EL^* \qquad (1)$$

where EL* is an isomerized form (most probably, a more tightly bound form) of the EL complex, and k_{+1}, k_{-1}, k_{+2}, and k_{-2} are the rate constants for the elementary processes as indicated in eq 1. For this mechanism, two relaxation times at the most can be expected, and the reciprocal of the slower relaxation time, k_{app}, is given, under the condition that $[L]_0 \gg [E]_0$, as follows (Halford, 1975):

$$k_{app} = \frac{k_{+2}[L]_0}{K_{-1} + [L]_0} + k_{-2} \qquad (2)$$

where K_{-1} is the dissociation constant of EL (the less tightly bound complex) defined as

$$K_{-1} = \frac{[E][L]}{[EL]} = \frac{k_{-1}}{k_{+1}} \qquad (3)$$

The values of k_{-2} can be obtainable in reasonable accuracy from the vertical intercept of the k_{app} vs. $[L]_0$ plot, by linear extrapolation in low $[L]_0$ region. When the k_{-2} value thus determined was used, K_{-1} and k_{+2} were evaluated by the

Table I: Thermodynamic and Activation Parameters for the Elementary Processes in the Binding of Gluconolactone to the Enzyme (pH 4.5, 10 °C)[a]

process	ΔG° kJ mol^{-1}	ΔG° kcal mol^{-1}	ΔH° kJ mol^{-1}	ΔH° kcal mol^{-1}	ΔS° J mol^{-1} deg^{-1}	ΔS° eu
bimolecular ($E + L \rightleftarrows EL$)	−9.4 ± 0.1	−2.24 ± 0.01	−14.5 ± 3.5	−3.5 ± 1.4	17.1 ± 11.7	4.07 ± 2.8
unimolecular ($EL \rightleftarrows EL^*$)	−5.5 ± 0.9	−1.3 ± 0.2	−29.2 ± 2.7	−7.0 ± 0.6	−79.7 ± 9.9	−19.1 ± 2.4

process	E_a kJ mol^{-1}	E_a kcal mol^{-1}	$\Delta G^\ddagger$ kJ mol^{-1}	$\Delta G^\ddagger$ kcal mol^{-1}	$\Delta H^\ddagger$ kJ mol^{-1}	$\Delta H^\ddagger$ kcal mol^{-1}	$\Delta S^\ddagger$ J mol^{-1} deg^{-1}	$\Delta S^\ddagger$ eu
k_{+2} step	47.6 ± 2.5	11.4 ± 0.6	56.0 ± 0.9	13.4 ± 0.2	45.1 ± 2.5	10.8 ± 0.6	−36.7 ± 8.9	−8.8 ± 2.1
k_{-2} step	76.8 ± 0.9	18.4 ± 0.2	61.5 ± 0.3	14.7 ± 0.1	74.3 ± 0.9	17.8 ± 0.2	43.0 ± 3.0	10.3 ± 0.7

[a] The values are means ± the standard deviation. ΔG°, ΔH°, and ΔS° are the standard Gibbs energy change, the standard enthalpy change, and the standard entropy change, respectively. E_a is the Arrhenius activation energy obtained experimentally. $\Delta G^\ddagger$, $\Delta H^\ddagger$, and $\Delta S^\ddagger$ represent the Gibbs energy, the enthalpy, and the entropy, of activation, respectively. These values are calculated from the activation parameters for the k_{+2} and k_{-2} steps.

nonlinear least-squares method (Sakoda & Hiromi, 1976) based on the rearranged form of eq 2:

$$k_{app} - k_{-2} = \frac{k_{+2}[L]_0}{K_{-1} + [L]_0} \quad (4)$$

The solid line in Figure 2 is a theoretical curve drawn with eq 2 using the following values thus obtained: K_{-1} = 14.3 ± 1.7 mM, k_{+2} = 348 ± 18 s^{-1}, and k_{-2} = 22.2 ± 3.2 s^{-1}. The values are means ± the standard deviation.

The signal amplitude, i.e., the fluorescence intensity decrease observed by the stopped-flow method, can give useful information concerning the nature of the processes involved (Nakatani & Hiromi, 1980). If we define ΔF_{SF} as the total fluorescence intensity decrease of the relaxation which would be observed when the dead time of the apparatus is zero, ΔF_{SF} can be estimated by (Ohnishi & Hiromi, 1978; Hiromi, 1979)

$$\Delta F_{SF} = \Delta F_{obsd} \exp(k_{app} t_d) \quad (5)$$

where ΔF_{obsd} is the fluorescence intensity decrease actually observed in the stopped-flow apparatus having a dead time t_d. By comparing ΔF_{SF} with the overall fluorescence decrease obtained by the static titration method ΔF_{static} (Hiromi et al., 1981), we can assign the degree of fluorescence intensity decrease to each process involved in eq 1. Figure 3 shows the comparison of ΔF_{static} with ΔF_{SF}. In the figure, open circles show ΔF_{SF} expressed as a percentage of the fluorescence intensity decrease relative to the fluorescence intensity of the free enzyme, which can be obtained by mixing the enzyme solution with the buffer instead of the gluconolactone solution in the stopped-flow apparatus. The solid curve in Figure 3 shows the theoretical curve obtained by the static method described in the preceding paper (Hiromi et al., 1981). Since the obtained fluorescence decrease refers to the slower relaxation expectable from the two-step mechanism (eq 1), the good agreement between ΔF_{SF} and ΔF_{static} indicates that the fluorescence intensity decrease occurs solely in the unimolecular process.

In the two-step mechanism, the overall dissociation constant K_d for the enzyme–gluconolactone complex is represented as

$$K_d = \frac{[E][L]}{[EL] + [EL^*]} = \frac{K_{-1}}{1 + (k_{+2}/k_{-2})} \quad (6)$$

With the values kinetically obtained for k_{+2}, k_{-2}, and K_{-1}, the value of K_d is calculated to be 0.93 mM, which is in good agreement with that obtained by the static method (1.1 mM) (Hiromi et al., 1981).

Thermodynamic and Activation Parameters for the Binding of Gluconolactone to the Enzyme. The temperature dependences of K_{-1}, k_{+2}, and k_{-2} of the gluconolactone binding were studied by the stopped-flow method between 0.5 and 30 °C. Figure 4a shows the Arrhenius plot of k_{+2}. From its slope, the activation energy E_a for the k_{+2} step in eq 1 was determined to be 47.6 ± 2.5 kJ/mol (11.4 ± 0.6 kcal/mol). Other activation parameters, $\Delta G^\ddagger$, $\Delta H^\ddagger$, and $\Delta S^\ddagger$ for the k_{+2} step can be obtained therefrom. The activation parameters for the k_{-2} step and the thermodynamic parameters for the bimolecular process in eq 1 were determined on the basis of the Arrhenius plot of k_{-2} (Figure 4b) and the van't Hoff plot of K_{-1} (Figure 4c), respectively.

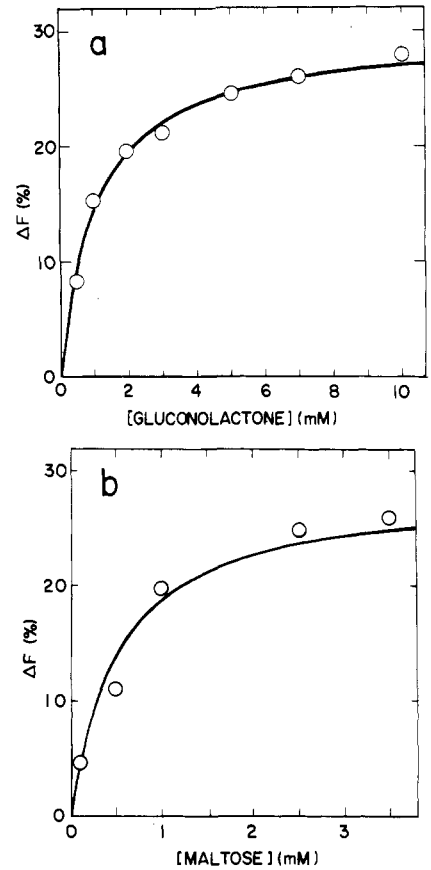

FIGURE 3: Comparisons of the fluorescence intensity decrease ΔF observed by the static method, ΔF_{static}, with that observed by the stopped-flow method, ΔF_{SF}, for the enzyme–gluconolactone system (a) and the enzyme–maltose system (b). The solid lines are the theoretical curves of ΔF_{static} based on the fluorometric titration (Hiromi et al., 1981) (static observation), and the open circles represent the ΔF_{SF} (kinetic observation) obtained from the stopped-flow study which was corrected for the dead time (see text).

Table I summarizes the thermodynamic parameters for the bimolecular and the unimolecular processes and the activation

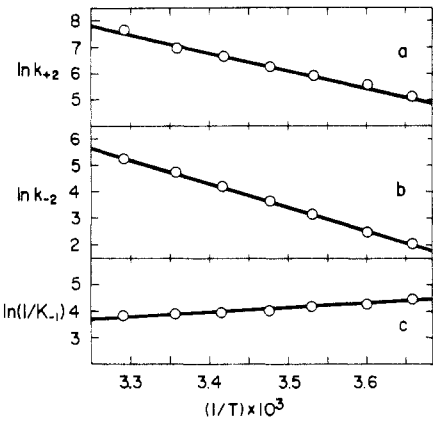

FIGURE 4: Temperature dependence of the kinetic parameters for the binding of gluconolactone to the enzyme, pH 4.5. (a) Arrhenius plot of k_{+2}. (b) Arrhenius plot of k_{-2}. (c) van't Hoff plot of K_{-1}.

parameters of the forward (k_{+2}) and backward (k_{-2}) steps of the unimolecular process. The thermodynamic parameters of the unimolecular process in Table I were calculated by using the activation parameters for the k_{+2} and k_{-2} steps.

Binding of a Substrate Maltose to Glucoamylase. The binding kinetics of the enzyme with a substrate maltose was also studied by the fluorescence stopped-flow method in a similar manner but at the temperature of 5 °C. Figure 1b shows an example of the reaction curves obtained by the stopped-flow method. The apparent first-order rate constant k_{app} of the binding reaction was obtained by the same procedure as for gluconolactone. The plot of k_{app} against the initial concentration of maltose $[M]_0$ is shown in Figure 2b. Obviously, the dependence of k_{app} on $[M]_0$ is hyperbolic, and the two-step mechanism of eq 1 type can be suggested also for the binding reaction of maltose:

$$E + M \underset{k_{-1}}{\overset{k_{+1}}{\rightleftharpoons}} EM \underset{k_{-2}}{\overset{k_{+2}}{\rightleftharpoons}} EM^* \qquad (7)$$

where M, EM, and EM* are maltose, the enzyme–maltose complex, and the isomerized form of the complex, respectively. The reciprocal of the slower relaxation time, k_{app}, is given, under the condition that $[M]_0 \gg [E]_0$, as

$$k_{app} = \frac{k_{+2}[M]_0}{K_{-1} + [M]_0} + k_{-2} \qquad (8)$$

From the plot of Figure 2b, the constants K_{-1}, k_{+2}, and k_{-2} were evaluated to be 5.61 ± 0.6 mM, 2030 ± 80 s^{-1}, and 45.1 ± 3.3 s^{-1}, respectively, by the same procedure as in the case of gluconolactone. The solid line in Figure 2b shows the theoretical curve obtained from eq 8 with the above values.

The fluorescence intensity decrease observed by the stopped-flow method (corrected for the dead time of the apparatus), ΔF_{SF} (open circules in Figure 3b), was almost equal to ΔF_{static} obtained by the static method (solid line in Figure 3b). This result indicates that the fluorescence intensity decrease occurs solely in the unimolecular process, as in the case of gluconolactone.

Influence of Glucose on the Binding Kinetics of Gluconolactone and Maltose with the Enzyme.[2] In the presence of glucose, the binding reactions of gluconolactone and maltose to the enzyme were found to be retarded considerably. Parts

[2] The binding of glucose with the enzyme was found to be too fast to be observed by the present stopped-flow technique. In the analysis of the kinetic studies in this paper, therefore, we can use rapid equilibrium approximation for the binding of the enzyme and glucose, as will be described later.

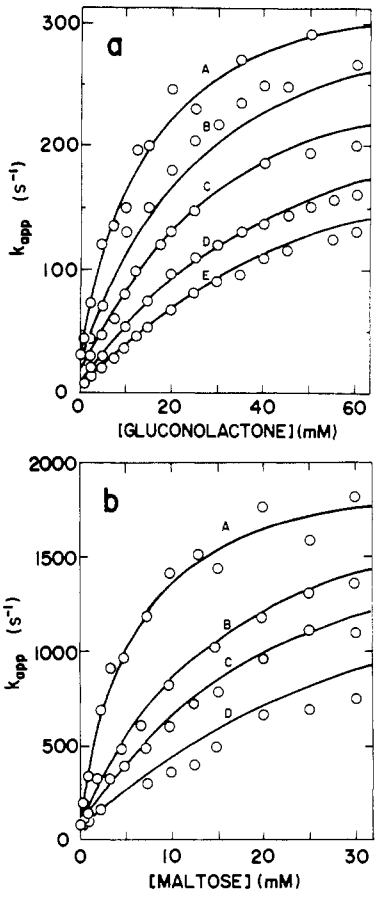

FIGURE 5: Dependence of k_{app} on the initial concentration of gluconolactone (a) and maltose (b) in the presence of various concentrations of glucose. (a) $[Glucoamylase]_0$ = 6.1 μM and $[glucose]_0$ = 0 (A), 50 (B), 100 (C), 200 (D), and 250 mM (E) at pH 4.5, 10 °C; (b) $[glucoamylase]_0$ = 13.1 μM and $[glucose]_0$ = 0 (A), 50 (B), 100 (C), and 200 mM (D) at pH 4.5, 5 °C. The solid lines are the theoretical curves (see Discussion).

a and b of Figure 5 show the dependence of k_{app} on the initial concentrations of gluconolactone and maltose, respectively, in the presence of various concentrations of glucose. The solid lines in these figures are the theoretical curves, which will be described under Discussion. For each case, the apparent values of the rate parameters, K_{-1}, k_{+2}, and k_{-2}, termed as $(K_{-1})_{app}$, $(k_{+2})_{app}$, and $(k_{-2})_{app}$, respectively, were evaluated. Parts a and b of Figure 6 show the dependences of these rate parameters of the enzyme–gluconolactone system and of the enzyme–maltose system on the initial concentration of glucose.

From these figures, the following points should be noted: (1) For both of the enzyme–gluconolactone and the enzyme–maltose systems, the value of $(K_{-1})_{app}$ almost linearly increases with increasing glucose concentration (Figure 6a-i,b-i). Obviously glucose inhibits the fast bimolecular processes of these binding reactions. (2) For both of the systems, the values of $(k_{+2})_{app}$ are almost independent of the concentration of glucose (Figure 6a-ii,b-ii). Glucose does not seem to inhibit the forward unimolecular process (k_{+2} step) significantly of either the gluconolactone or maltose binding. (3) The effect of glucose on the k_{-2} step is quite different for the gluconolactone and maltose systems. The value of $(k_{-2})_{app}$ of the enzyme–maltose system is independent of the concentration of glucose (Figure 6b-iii) whereas that of the enzyme–gluconolactone system is remarkably decreased by the addition of glucose (Figure 6a-iii). This implies that glucose inhibits the backward unimolecular process (k_{-2} step) of the enzyme–gluconolactone system whereas it does not inhibit the same process of the enzyme–maltose system.

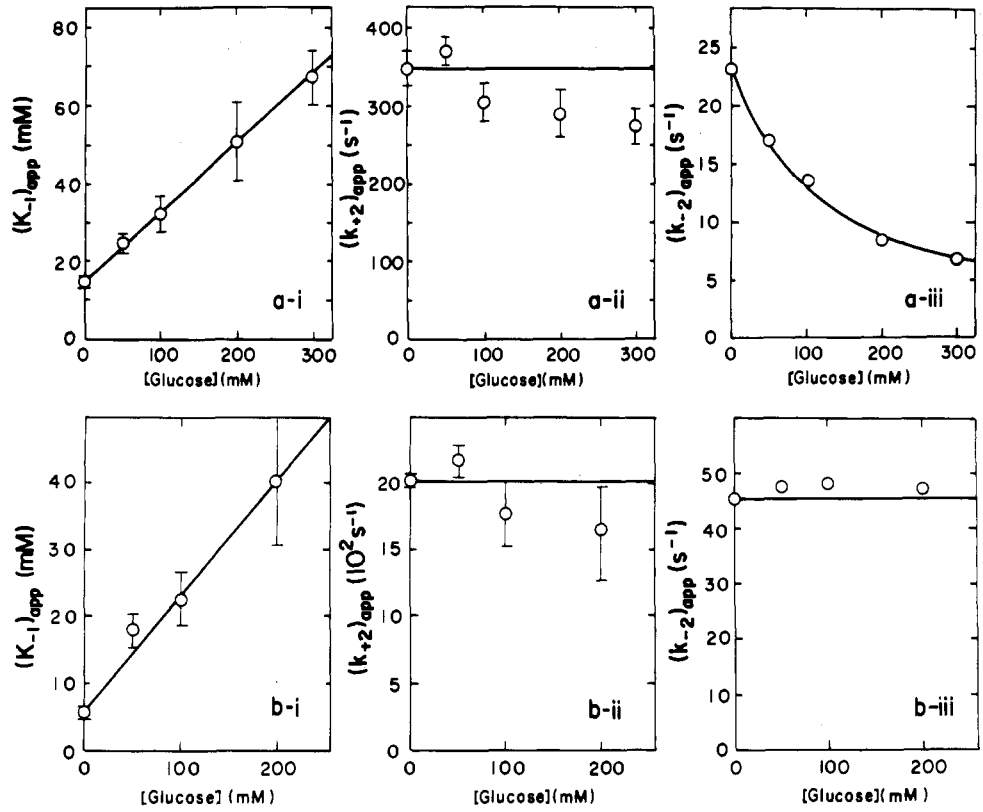

FIGURE 6: Effect of glucose concentration on the kinetic parameters $(K_{-1})_{app}$, $(k_{+2})_{app}$, and $(k_{-2})_{app}$ for the binding of the enzyme with gluconolactone (a) and maltose (b). The solid lines were drawn according to the following equations: $(K_{-1})_{app} = K_{-1}[1 + ([G]_0/K_G)]$ (a-i and b-i), $(k_{+2})_{app} = k_{+2}$ (a-ii and b-ii), $(k_{-2})_{app} = k_{-2}/[1 + ([G]_0/K_G')]$ (a-iii), and $(k_{-2})_{app} = k_{-2}$ (b-iii), using $K_{-1} = 14.3$ mM, $K_G = 81.1$ mM, $K_G' = 120$ mM, $k_{+2} = 348$ s^{-1}, and $k_{-2} = 22.2$ s^{-1} (a-i–iii) and $K_{-1} = 5.61$ mM, $K_G = 35$ mM, $k_{+2} = 2030$ s^{-1}, and $k_{-2} = 45.1$ s^{-1} (b-i–iii) (cf. eq 10, 11, and 13).

Discussion

In the enzyme–ligand interaction, a hyperbolic concentration dependence of k_{app}, such as shown in Figure 2, is rather commonly observed (Hammes & Schimmel, 1970; Hiromi, 1979). This kinetic feature is consistent with the two-step mechanism which involves a fast bimolecular process and a subsequent unimolecular "isomerization" process. The nature of the isomerization process could be relocation of the ligand on the enzyme or a conformation change in enzyme and/or ligand (Hammes & Schimmel, 1970; Halford, 1975; Hiromi, 1979).

The analysis of signal amplitudes obtained from the stopped-flow studies is useful to infer the microscopic molecular mechanism when combined with the information obtained from static studies (Nakatani & Hiromi, 1980). In the following sections, we discuss the binding process of the gluconolactone and maltose to the enzyme in the presence of glucose.

Binding Process of Gluconolactone to the Enzyme. As was mentioned earlier, it is reasonable to assume that gluconolactone binds to subsite 1 of the enzyme and glucose predominantly binds to subsite 2 (cf. Figure 1 in the preceding paper). Moreover, it is reasonably concluded that the tryptophan residue giving rise to the difference spectrum and the fluorescence intensity decrease is most probably located at subsite 1, on the basis of the above-mentioned static studies (Ohnishi et al., 1975; Hiromi et al., 1981) and the transient kinetics for the chemical modification of the enzyme with *N*-bromosuccinimide (M. Taniguchi et al., unpublished results).

It is quite reasonable to consider that the enzyme–gluconolactone complex observed by the static fluorometry (Hiromi et al., 1981) corresponds mostly to EL* in eq 1, since the equilibrium of the unimolecular process in eq 1 (EL ⇄ EL*) inclines toward the EL* complex ($k_{+2}/k_{-2} = 15.9$), and hence, the dissociation constant of the EL complex, K_{-1} (14 mM), is significantly greater than the overall dissociation constant ($K_d = 1.1$ mM).

Thus, the characteristic of the gluconolactone binding may be summarized as follows: (1) Gluconolactone binds to the enzyme in a two-step mechanism:

$$E + L \underset{K_{-1}}{\rightleftharpoons} EL \underset{k_{-2}}{\overset{k_{+2}}{\rightleftharpoons}} EL^*$$

(2) The fluorescence intensity decrease occurs solely in the unimolecular process (EL ⇄ EL*) but not in the bimolecular process (E + L ⇄ EL). (3) The tryptophan residue responsible for the fluorescence intensity decrease is probably located at subsite 1. (4) Gluconolactone is bound at subsite 1 in the final state (EL*). (5) Glucose, which predominantly binds to subsite 2, inhibits the bimolecular process and the backward unimolecular process (k_{-2} step) of gluconolactone binding.

From these points, we propose the following mechanism for gluconolactone binding. Gluconolactone binds transiently to subsite 2 in the bimolecular process to form the EL complex ($K_{-1} = 14$ mM), and then gluconolactone relocates to subsite 1 in the slow unimolecular process to form the stable EL* complex ($K_d = 1.1$ mM), as is schematically shown in Figure 7a. In this mechanism, glucose (G), which binds to subsite 2, can bind both to the free enzyme and to the EL* complex. In the presence of glucose, the relevant mechanism is given as

$$\begin{array}{ccccc} E & + & L & \underset{k_{-1}}{\overset{k_{+1}}{\rightleftharpoons}} & EL \underset{k_{-2}}{\overset{k_{+2}}{\rightleftharpoons}} EL^* \\ + & & & & + \\ G & & & & G \\ \Vert\uparrow\downarrow K_G & & & & \Vert\uparrow\downarrow K_G' \\ EG & & & & EGL^* \end{array} \qquad (9)$$

K_G and K_G' are dissociation constants defined as $K_G = [E][G]/[EG]$ and $K_G' = [EL^*][G]/[EGL^*]$. Since the detailed binding mechanism of glucose is not clear at present, we temporarily assume a single-step mechanism and the rapid equilibrium for the binding of glucose to subsite 2 of the enzyme. The rapid equilibrium approximation seems to be rational since the binding of glucose to the enzyme is too fast to be observed by the stopped-flow apparatus (See footnote 2).

Then for gluconolactone binding in the presence of glucose, when $[L]_0$ and $[G]_0$ are much greater than $[E]_0$, k_{app} is given as

$$k_{app} = \frac{k_{+2}[L]_0}{K_{-1}[1 + ([G]_0/K_G)] + [L]_0} + \frac{k_{-2}}{1 + ([G]_0/K_G')} \quad (10)$$

$$\equiv \frac{k_{+2}[L]_0}{(K_{-1})_{app} + [L]_0} + (k_{+2})_{app} \quad (11)$$

where $(K_{-1})_{app} = K_{-1}[1 + ([G]_0/K_G)]$ and $(k_{-2})_{app} = k_{-2}/[1 + ([G]_0/K_G')]$. According to eq 10, the slope in Figure 6a-i $[(K_{-1})_{app}$ vs. $[G]_0$ plot] represents K_{-1}/K_G, from which the value of K_G was determined to be 81.1 ± 2.1 mM (10 °C) by using the value of K_{-1} = 14.3 mM. The value of K_G thus obtained is comparable with 130 mM, which was obtained from the fluorometric titration at 10 °C (Hiromi et al., 1981), and with 50 mM, obtained from the UV difference absorption spectrum titration at 25 °C (Ohnishi et al., 1975). The K_G' value, obtained from the glucose concentration which gives one-half of $(k_{-2})_{app}$ at $[G]_0$ = 0 mM in Figure 6a-iii, is 120 mM, which is of the same order of magnitude as that obtained from the fluorometric titration (58 mM) (Hiromi et al., 1981).

Binding Process of Maltose to the Enzyme. In a similar manner, the following mechanism can be proposed for the binding of maltose. Maltose binds transiently to subsites 2 and 3 in the bimolecular process to form the EM complex (K_{-1} = 5.6 mM) and relocates then to subsites 1 and 2 to form the EM complex (K_d = 0.5 mM). In this model, glucose can bind only to the free enzyme, since subsite 2 in both of the EM and EM* complexes are occupied by the nonreducing-end and reducing-end glucose residues of maltose, respectively (Figure 7b). The mechanism for maltose binding in the presence of glucose is thus given as

$$\begin{array}{ccccc} E & + M & \underset{k_{-1}}{\overset{k_{+1}}{\rightleftharpoons}} & EM & \underset{k_{-2}}{\overset{k_{+2}}{\rightleftharpoons}} EM^* \\ + & & & & \\ G & & & & \\ \Big\downarrow\uparrow K_G & & & & \\ EG & & & & \end{array} \quad (12)$$

k_{app} for maltose binding is given by

$$k_{app} = \frac{k_{+2}[M]_0}{K_{-1}[1 + ([G]_0/K_G)] + [M]_0} + k_{-2} \quad (13)$$

From the slope in Figure 6b-i $[(K_{-1})_{app}$ vs. $[G]_0$ plot], the value of K_G was determined to be 35.1 ± 0.5 mM (5 °C). The K_G value thus obtained is satisfactorily consistent with those mentioned above, considering the possible error involved in the estimation.

Comparison between the Theoretical and the Experimental Results. On the basis of the mechanism proposed in eq 9 and 12, by using eq 10 and 13 and the values of the constants K_{-1}, k_{+2}, k_{-2}, K_G, and K_G', we can theoretically reproduce the dependence of k_{app} on the initial concentration of gluconolactone and maltose in the presence of glucose. Parts a and b of Figure 5 show the comparison of the theoretical curves with the experimental ones; circles represent the experimental data and the solid lines the theroetical curves thus obtained. As seen in Figure 5, the agreement between the theoretical curves and the experimental data is satisfactory, indicating that the proposed models (Figure 7) and the mechanisms (eq 9 and 12) are suitable for describing the binding of gluconolactone and maltose.

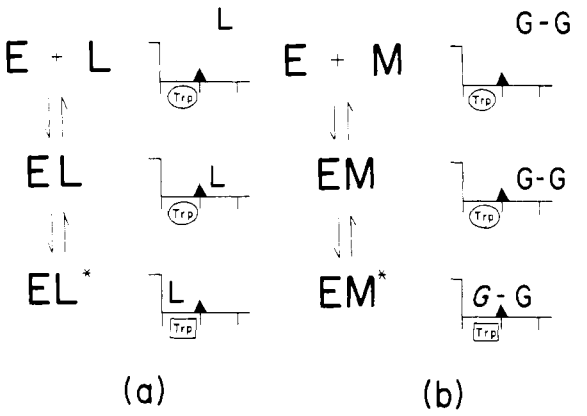

FIGURE 7: Proposed mechanisms of the binding processes of gluconolactone (a) and maltose (b). The wedge indicates the catalytic site. (Trp) and [Trp] indicate the emissive and the quenched states of the tryptophan fluorescence, respectively.

In summary, gluconolactone and maltose are considered to bind to the enzyme in a two-step mechanism consisting of a fast bimolecular process and a subsequent slow unimolecular isomerization process. The fluorescence intensity decrease is accompanied solely with the unimolecular process for each ligand. The nature of the unimolecular isomerization process may probably be a relocation of the ligands on the enzyme, i.e., relocation from subsite 2 to subsite 1 for gluconolactone and from subsites 2 and 3 to subsites 1 and 2 for maltose.

References

Bernasconi, C. F. (1976) *Relaxation Kinetics*, pp 20–39, Academic Press, New York.

Eigen, M., & DeMayer, L. (1963) *Tech. Org. Chem. 8 (Part 2)*, 895–1054.

Guggenheim, E. A. (1926) *Philos. Mag. 2*, 538–543.

Halford, S. E. (1975) *Biochem. J. 149*, 411–422.

Hammes, G. G., & Schimmel, P. R. (1970) *Enzymes, 3rd Ed., 2*, 67–114.

Hiromi, K. (1970) *Biochem. Biophys. Res. Commun. 40*, 1–6.

Hiromi, K. (1979) *Kinetics of Fast Enzyme Reactions: Theory and Practice*, Kodansha Ltd., Halsted Press, Tokyo, New York.

Hiromi, K., Nitta, Y., Numata, C., & Ono, S. (1973) *Biochim. Biophys. Acta 302*, 362–375.

Hiromi, K., Ohnishi, M., & Yamashita, T. (1974) *J. Biochem. (Tokyo) 76*, 1365–1367.

Hiromi, K, Tanaka, A, & Ohnishi, M. (1981) *Biochemistry* (preceding paper in this issue).

Nakatani, H., & Hiromi, K. (1980) *J. Biochem. (Tokyo) 87*, 1805–1810.

Ohnishi, M., & Hiromi, K. (1978) *Carbohydr. Res. 61*, 335–344.

Ohnishi, M., Kegai, H., & Hiromi, K. (1975) *J. Biochem. (Tokyo) 77*, 695–703.

Ohnishi, M., Yamashita, T., & Hiromi, K. (1977) *J. Biochem. (Tokyo) 81*, 99–105.

Robyt, J. F., & French, D. (1963) *Arch. Biochem. Biophys. 100*, 451–467.
Sakoda, M., & Hiromi, K. (1976) *J. Biochem. (Tokyo) 80*, 547–555.
Shimahara, K., & Takahashi, T. (1970) *Biochim. Biophys. Acta 201*, 410–415.
Tonomura, B., Nakatani, H., Ohnishi, M., Yamaguchi-Ito, J., & Hiromi, K. (1978) *Anal. Biophys. 84*, 370–383.

Kinetic Studies To Determine the Mechanism of Regulation of Bovine Liver Glutamate Dehydrogenase by Nucleotide Effectors†

Paul F. Cook

ABSTRACT: A combination of kinetic and isotope effect studies in the presence and absence of the effectors ADP and GTP was used to elucidate the mechanism of regulation of bovine liver glutamate dehydrogenase. ADP at low concentrations of glutamate competes with TPN for free enzyme. GTP exhibits a similar effect at high concentrations (100 μM and above). When ADP binds at its allosteric site, it increases the off rates of both α-ketoglutarate and TPNH from their product complexes. This results in a decrease in V/K for both substrates, an increase in V, and an increase in the deuterium isotope effects for all three parameters so that they are all about 1.3. The rate of release of glutamate from E–TPNH–glutamate is also apparently enhanced since no substrate inhibition by glutamate is observed in the presence of ADP. The effect of GTP is in opposition to that of ADP in that GTP decreases the off rates for both TPN and glutamate from E–TPN–glutamate as well as the off rates for α-ketoglutarate and TPNH. This results in an increase in the V/K's for both substrates, a decrease in V, and a decrease in the deuterium isotope effects for all three parameters to a value of 1. Substrate inhibition by glutamate is also eliminated by GTP probably by preventing any significant accumulation of E–TPNH to which glutamate binds as an inhibitor.

Glutamate dehydrogenase catalyzes the reversible oxidative deamination of L-glutamate by TPN to TPNH, α-ketoglutarate, and ammonia. Frieden (1959) has shown that this enzyme is regulated allosterically by nucleotides. Activation is obtained with the nucleoside diphosphates ADP and GDP while inhibition is obtained with ATP and GTP.

The nucleoside diphosphates have been found to enhance the rate of formation of a dead-end E–TPNH–glutamate complex and inhibit the formation of the E–TPNH–α-ketoglutarate complex (Sanner, 1975) probably by increasing the off rate for α-ketoglutarate from this complex (Andree, 1978). Dalziel & Egan (1972) have shown that in the presence of 1 mM ADP, TPN does not bind at all in the absence of glutamate. In opposition, the nucleoside triphosphates inhibit the rate of formation of E–TPNH–glutamate and enhance the formation of the E–TPNH–α-ketoglutarate complex (Sanner, 1975) presumably by decreasing product off rates (di Franco, 1974). In addition, 0.8 mM GTP enhances the binding of TPN to free enzyme (Dalziel & Egan, 1972).

More recently, George & Bell (1980) have shown that ADP is a competitive inhibitor of TPN at low concentrations of glutamate. In addition, these authors have shown that ADP activates by destabilizing the E–TPNH–glutamate complex. Modification of a single imidazole residue by diethyl pyrocarbonate treatment yields an activation similar to that observed with ADP.

This paper presents studies which indicate that the mechanism of activation of an enzyme can best be determined by a complete and systematic study of the effect of modifiers on each of the kinetic parameters. Once these have been determined, results may be tested, if possible by the use of deuterium isotope effects.

† From the Department of Biochemistry, Louisiana State University Medical Center, New Orleans, Louisiana 70112. *Received June 15, 1981.*

Materials and Methods

Chemicals. Bovine liver glutamate dehydrogenase was obtained from Sigma. L-Glutamate-*2-d* was prepared by the method of Rife & Cleland (1980). All other reagents were obtained from commercial sources and were of the best quality available. Glutamate concentrations were determined enzymatically according to Cook et al. (1980).

Initial Velocity Studies. Initial velocity studies were carried out with a Beckman DU monochromator and a Gilford OD converter by monitoring the change in absorbance at 340 nm due to production of TPNH. All studies were carried out at pH 7.1 in 70 mM phosphate buffer. Ionic strength was maintained at 0.4 M by addition of NaCl.

Data Processing. Reciprocal initial velocities were plotted against reciprocal substrate concentrations, and all plots were linear except those in the absence of either GTP or ADP which exhibited substrate inhibition by glutamate. The data were fitted to appropriate equations with the FORTRAN programs of Cleland (1979). The initial velocity pattern obtained in the absence of GTP or ADP was fitted to eq 1, while all other

$$v = \frac{VAB}{K_{ia}K_b + K_bA + K_aB + AB(1 + B/K_{II})} \quad (1)$$

$$v = \frac{VAB}{K_{ia}K_b + K_bA + K_aB + AB} \quad (2)$$

$$y = \frac{a(1 + P/K_{I\,num})}{1 + P/K_{I\,denom}} \quad (3)$$

$$y = mx + b \quad (4)$$

$$v = \frac{VA}{K_a(1 + F_iE_{V/K}) + A(1 + F_iE_V)} \quad (5)$$

initial velocity patterns were fitted to eq 2. Hyperbolic functions of kinetic parameters vs. ADP and GTP concentrations were fitted to eq 3. Linear functions of kinetic parameters vs. ADP concentration were fitted to eq 4. All data

0006-2960/82/0421-0113$01.25/0